Cell, Vol. 103, 75–85, September 29, 2000, Copyright ©2000 by Cell Press

Combinatorial Signaling in the Specification of Unique Cell Fates

Gail V. Flores,[1,7] Hong Duan,[2,5,7] Huajun Yan,[1,7] Raghavendra Nagaraj,[1,7] Weimin Fu,[2,6] Yu Zou,[2] Markus Noll,[2] and Utpal Banerjee[1,3,4]

[1] Department of Molecular, Cell, and Developmental Biology and Molecular Biology Institute
University of California at Los Angeles
Los Angeles, California 90095

[2] Institute for Molecular Biology
University of Zürich
CH-8057 Zürich
Switzerland

[3] Department of Biological Chemistry and Department of Human Genetics
University of California at Los Angeles
Los Angeles, California 90095

Summary

How multifunctional signals combine to specify unique cell fates during pattern formation is not well understood. Here, we demonstrate that together with the transcription factor Lozenge, the nuclear effectors of the EGFR and Notch signaling pathways directly regulate *D-Pax2* transcription in cone cells of the *Drosophila* eye disc. Moreover, the specificity of *D-Pax2* expression can be altered upon genetic manipulation of these inputs. Thus, a relatively small number of temporally and spatially controlled signals received by a set of pluripotent cells can create the unique combinations of activated transcription factors required to regulate target genes and ultimately specify distinct cell fates within this group. We expect that similar mechanisms may specify pattern formation in vertebrate developmental systems that involve intercellular communication.

Introduction

How individual cells within an initially equivalent group acquire a multitude of distinct fates is a fundamental question in developmental biology. Understanding the interplay between intercellular signals and the context in which they are interpreted is the focus of this study. During *Drosophila* eye development, undifferentiated cells are patterned to yield ~800 facets, called ommatidia. Each ommatidium is comprised of eight photoreceptor neurons (R1–R8), four nonneuronal cone cells, three classes of pigment cells, and a bristle complex. Eye morphogenesis initiates during the third larval instar of development as a morphogenetic furrow sweeps across the disc from posterior to anterior (Ready et al., 1976). Cells within the furrow arrest in the G1 phase of the cell cycle (Wolff and Ready, 1991). These cells either emerge from the furrow as five-cell preclusters of R2–R5 and R8, or they undergo a synchronized round of mitosis that creates a new pool of undifferentiated precursors. In a second phase of morphogenesis, these new precursors are recruited into the developing ommatidia as R1, R6, R7, cone, pigment, and bristle cells (Ready et al., 1976; Wolff and Ready, 1991). This study investigates the molecular mechanisms that regulate pattern formation during this second phase of morphogenesis.

Early pioneering work (Ready et al., 1976; Lawrence and Green, 1979; Tomlinson and Ready, 1987) and later molecular analysis (reviewed by Zipursky and Rubin, 1994; Freeman, 1997) showed that the recruitment of ommatidial cells follows a nonclonal mechanism involving extensive cell–cell interactions. The Sevenless (Sev) receptor tyrosine kinase (RTK) signaling cascade was identified as a pathway involved in the determination of a single cell type, R7. This initially suggested that each cell type in the eye may be specified by its own unique signaling mechanism. However, it was later shown that Sev can induce a non-R7 fate when activated in other cells (Dickson et al., 1992), or when the R7 precursor ectopically expresses a transcription factor that specifies R2/R5 fate (Basler et al., 1990; Kimmel et al., 1990). Conversely, an activated version of another RTK, epidermal growth factor receptor (EGFR), can direct an R7 fate in the absence of Sev (Freeman, 1996). These results indicate that while the Sev signal is required as a triggering event in the differentiation of R7, the cell's identity is specified by other mechanisms.

Another signaling cascade, initiated by EGFR, plays many roles during eye morphogenesis. EGFR signaling causes inactivation of the ETS domain repressor Yan and activation of the ETS domain transcriptional activator PntP2 (Brunner et al., 1994; O'Neill et al., 1994; Rebay and Rubin, 1995). In addition to its requirement for the differentiation of all cell types in the eye (Freeman, 1996; Tio and Moses, 1997), the EGFR signal is essential for proper furrow initiation, proliferation, spacing, recruitment, and survival of cells in the eye disc (Baker and Rubin, 1989, 1992; Xu and Rubin, 1993; Freeman, 1996; Tio and Moses, 1997; Domínguez et al., 1998; Kumar et al., 1998; Lesokhin et al., 1999). While the EGFR signal has classically been considered instructive, this multitude of functions suggests that on its own, this pathway does not bear any fate-specifying information.

The Notch (N) signaling pathway also plays many roles in eye development through its activation of the transcription factor Suppressor of Hairless [Su(H)] (reviewed by Artavanis-Tsakonas et al., 1999). This pathway is required for the proper temporal acquisition of several cell fates in the eye (Cagan and Ready, 1989; Fortini et al., 1993), and also functions in proliferation, dorsal–ventral axis establishment, and ommatidial polarity (Domínguez and de Celis, 1998; Go et al., 1998; Papayannopoulos et al., 1998; Cooper and Bray, 1999; Fanto and Mlodzik, 1999). This variety of functions led to the characterization of N as a permissive signal and suggests that, like EGFR and Sev, the N signal alone cannot

[4] To whom correspondence should be addressed (e-mail: banerjee@mbi.ucla.edu).

[5] Present address: Department of Medicine, Division of Cardiology, Albert Einstein College of Medicine, Bronx, NY 10461.

[6] Present address: Department of Neurology, Northwestern University, Chicago, IL 60611.

[7] These authors contributed equally to this work.

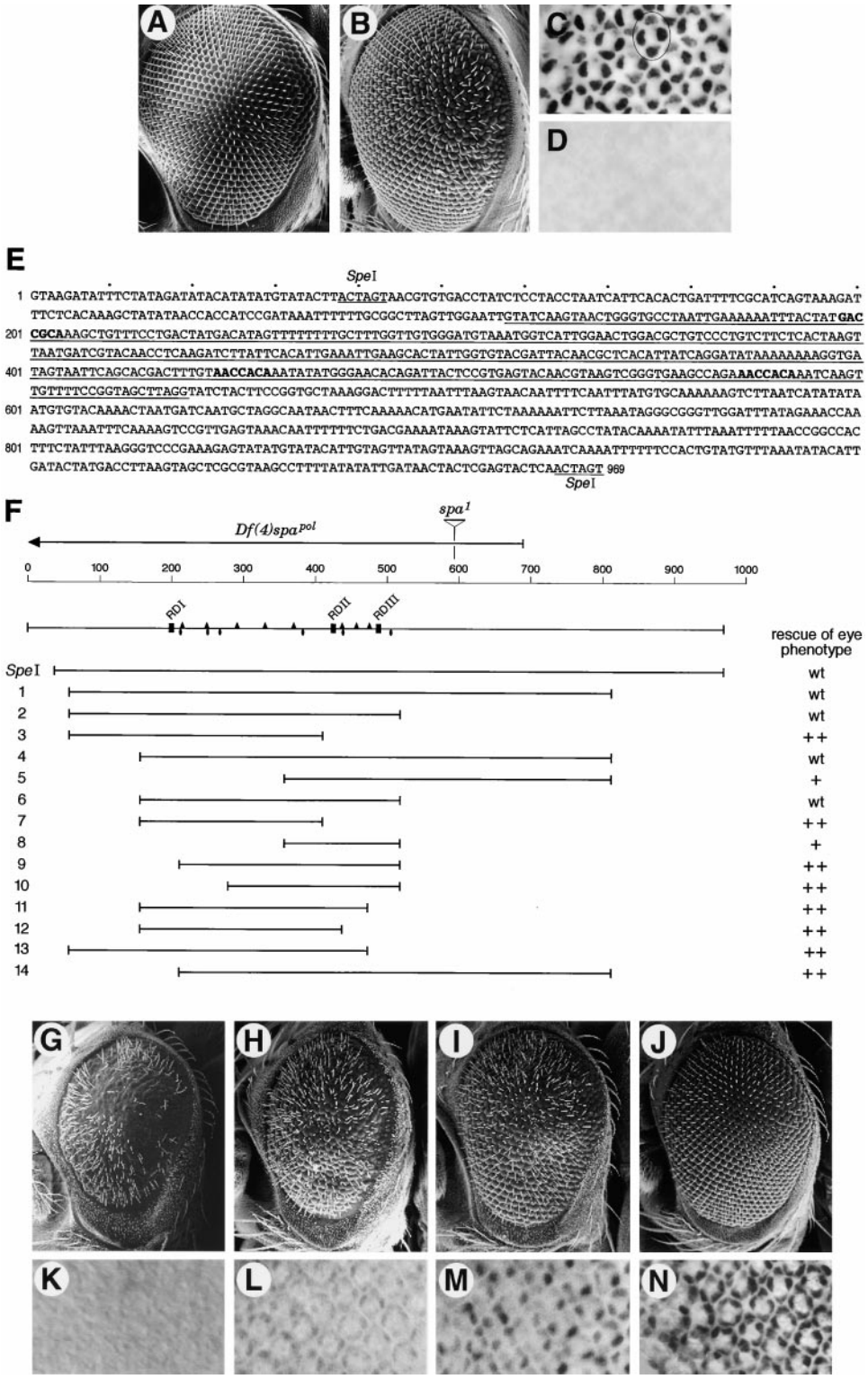

Figure 1. Identification of the Minimal *D-Pax2* Eye-Specific Enhancer and its Potential Lz/Runt Domain Binding Sites

Scanning electron micrographs (SEM) of adult eyes (A, B, and G–J) and immunolocalization of D-Pax2 in late third-instar larval eye discs (C, D, and K–N).

(A) lz^{ts1}/Y flies raised at 25°C. The eye phenotype is wild type.

(B) lz^{ts1}/Y; spa^{pol}/+ flies raised at 25°C. The eye-specific mutation spa^{pol} of *D-Pax2* dominantly enhances the lz^{ts1} phenotype.

(C) Wild type. D-Pax2 is expressed in four cone cell precursors per ommatidium (one example is circled).

(D) lz^{r1}. Note complete loss of D-Pax2 expression in cone cell precursors in this null *lz* allele.

(E) Sequence of *D-Pax2* that includes the eye-specific enhancer at the 5′ end of intron 4. The sequence begins with the splice donor site of

provide the unique information that is necessary to determine a specific cell fate. Each of these signaling cascades must therefore act as a trigger allowing a cell to choose one of several possible fates.

A panoply of transcription factors is expressed in specific cell types in the larval eye disc (reviewed by Freeman, 1997; Kumar and Moses, 1997). During the second phase of recruitment posterior to the furrow, Bar is expressed in R1/R6 (Higashijima et al., 1992), Prospero (Pros) in R7 and cone cells (Kauffmann et al., 1996), and D-Pax2 in cone and primary pigment cells (Fu and Noll, 1997). Combinations of such cell-specific transcription factors ultimately create the differences between cell types. However, their cell-specific expression patterns suggest that the initial discrimination between cell types is established prior to the onset of their expression. To understand cell fate specification, it is therefore important to elucidate the mechanisms involved in generating the unique expression patterns of these proteins. This was lacking in previous studies because controlling regions of these transcription factors had not yet been deciphered.

A first step toward unraveling cell fate specification mechanisms during the second phase of morphogenesis in the eye was the identification of the *lozenge* (*lz*) gene (Daga et al., 1996), which encodes a Runt Domain–containing transcription factor that shares sequences with *Drosophila* Runt and human AML1 (*A*cute *M*yeloid *L*eukemia 1), CBFA1, and CBFA3 (reviewed by Bae and Ito, 1999). Lz regulates the expression of all known cell-specific transcription factors expressed during the second phase of morphogenesis. In *lz* mutants, Bar (Daga et al., 1996; Crew et al., 1997), Pros (Xu et al., 2000 [this issue of *Cell*]), and D-Pax2 (this study) are not expressed, and Seven-up is ectopically expressed in R7 and cone cells (Daga et al., 1996; Crew et al., 1997). Since Lz is expressed in the entire pool of undifferentiated precursor cells posterior to the morphogenetic furrow (Flores et al., 1998), it remained unclear how it causes its target genes to be expressed in a cell-specific manner. Here, we describe results in support of a model for cell fate specification. Its salient feature is the combinatorial use by a cell of a small number of multifunctional signaling pathways controlling the activity of specific transcription factors to activate specific target genes at the appropriate time in development.

Results

Lozenge Directly Regulates *D-Pax2* Expression in Cone Cell Precursors

D-Pax2 is the *Drosophila* homolog of the vertebrate *Pax2* gene (Fu and Noll, 1997; Czerny et al., 1997). This locus is represented by at least two classes of mutant alleles, *shaven* (*sv*) and *sparkling* (*spa*) (Fu et al., 1998; Kavaler et al., 1999). *spa* mutants show cone cell defects resulting from mutations in the fourth intron of the gene, which led to the identification of a 926 bp SpeI fragment within this intron that includes the eye-specific enhancer (Fu and Noll, 1997) (Figure 1F). When combined with its promoter and coding region, this fragment restores wild-type D-Pax2 expression in cone cell precursors of *spa* mutants and rescues the *spa* eye phenotype (Fu et al., 1998).

Enhancement of *lz* eye phenotypes by *spa* alleles has been observed previously (Lindsley and Zimm, 1992; Gupta and Rodrigues, 1995). In addition, two new *spa* alleles were isolated as enhancers of the temperature-sensitive *lz* allele, lz^{ts1} (J. Kaminker, T. Lebestky, and U. B., unpublished data). The strongest eye-specific allele of *D-Pax2*, spa^{pol}, which is not transcribed in cone cell precursors (Fu and Noll, 1997), also enhances lz^{ts1} (Figures 1A and 1B). We found that D-Pax2 is not expressed in cone cell precursors of *lz* mutants (Figures 1C and 1D), which suggests that Lz regulates *D-Pax2* expression. There are three Lz/Runt domain (RD) binding sites (5′-RACCRCA-3′, R = purine; Kamachi et al., 1990) in the *D-Pax2* eye-specific enhancer (RDI–RDIII; Figures 1E and 1F). To determine whether these sites are required for proper *D-Pax2* expression, a series of smaller enhancer fragments derived from the SpeI fragment (1–5 in Figure 1F) was combined with the *D-Pax2* promoter and transcribed region from which introns 1–8 had been removed (see Fu et al., 1998) and tested as transgenes for their ability to rescue spa^{pol} mutants (Figures 1G–1N). There was no loss in rescue efficiency if the truncation did not eliminate any of the three RD binding sites (1, 2, and 4 in Figure 1F). However, if RDI was deleted (5 in Figure 1F), the rescue efficiency (Figure 1H) and D-Pax2 expression in cone cell precursors (Figure 1L) were considerably reduced, and rescue could not be improved by two copies of the transgene (not shown). Similarly, when both RDII and RDIII were removed (3 in Figure 1F), the rescue efficiency (Figure 1I)

intron 4 and ends with the second SpeI site. Runt domain (RD) binding sites are in boldface, and the minimal eye-specific enhancer (SME; positions 158–519 of intron 4) is underlined.

(F) The extent of $Df(4)spa^{pol}$ and the position of the spa^{1} insertion (Fu and Noll, 1997) are mapped relative to the 5′ end of intron 4 whose sequence is shown in (E). In addition to the three RD binding sites, the positions within the SME of eight putative Su(H) (triangles) and six ETS domain (ovals) binding sites are shown. Below, the extent of the 926 bp SpeI fragment of intron 4 and of constructs 1–14 including the entire or truncated forms of the SME are indicated. Transformant lines carrying constructs 1–14 driving D-Pax2 expression were assessed for their efficiency to rescue the spa^{pol} adult eye phenotype. Construct 6 is the smallest enhancer fragment that can fully rescue (wt) spa^{pol}, while constructs 5 and 8 can only weakly rescue (+) and constructs 3, 7, and 9–14 can partially rescue (++) as single-copy transgenes. If homozygous viable, transgenes of constructs 3, 7, and 9–14 can fully rescue the eye phenotype whereas transgenes of constructs 5 and 8 cannot (not shown). The rescue efficiencies (+, ++, wt) indicated on the right are the average of many independent lines of each construct (see Experimental Procedures). Scale indicates distance in bp from the 5′ end of intron 4 of *D-Pax2*.

(G and K) spa^{pol}. Note roughening across entire eye (G) and lack of D-Pax2 expression in cone cell precursors (K).

(H and L) w^{1118}; *P[construct 5-D-Pax2,* w^{+}*]/+*; spa^{pol}. Construct 5, which lacks RDI, can only weakly rescue (+) the spa^{pol} phenotype (H) as well as D-Pax2 expression in cone cell precursors (L).

(I and M) w^{1118}; *P[construct 3-D-Pax2,* w^{+}*]/+*; spa^{pol}. Construct 3, which lacks RDII and RDIII, allows partial rescue (++) of the spa^{pol} phenotype (I) and D-Pax2 expression in cone cell precursors when present as a single copy (M).

(J and N) w^{1118}; *P[construct 6-D-Pax2,* w^{+}*]*; spa^{pol}. Construct 6 is the minimal enhancer fragment (SME) able to completely rescue the spa^{pol} phenotype (J) and D-Pax2 expression in cone cell precursors (N) when driving *D-Pax2* expression as a single-copy transgene.

and expression in cone cell precursors (Figure 1M) were clearly reduced, but rescue to wild type was achieved with two copies of the transgene (not shown). These experiments suggest that the RD binding sites are essential for the control of *D-Pax2* transcription and that omission of RDI has more severe effects than that of RDII and RDIII.

Construct 6, which extends from nucleotides 158–519 and contains all three RD sites (Figures 1E and 1F), is the smallest fragment that can rescue the *spa^{pol}* eye phenotype to wild type (Figure 1J) and D-Pax2 expression in cone cell precursors (Figure 1N) as a single-copy transgene; hence, it was designated as the *spa* minimal enhancer (SME). Any further truncation of this enhancer fragment that removes at least one of the three RD binding sites (7–12 in Figure 1F) destroys its ability to completely rescue the *spa^{pol}* phenotype by a single copy of the corresponding transgene. Eliminating only RDIII (11 and 12 in Figure 1F) or RDII and RDIII (7 in Figure 1F) has similar effects in that the corresponding transgenes in most lines are unable to rescue the *spa^{pol}* eye phenotype completely when present as single copies while the presence of two copies results in a wild-type eye phenotype (not shown). The same result is observed if only RDI is deleted (9 and 10 in Figure 1F). When, in addition, more than half of the SME is removed (8 in Figure 1F), the rescue efficiency is further reduced, which suggests that regulatory elements other than the RD sites are important in the SME. As these sequences are also eliminated in 5 (Figure 1F), it is likely that the reduced rescue efficiency of this fragment is caused by the deletion of sequences in addition to RDI. Sequences outside of the SME are unable to compensate for the loss of regulatory elements within the SME (cf. 13 with 11 or 3 with 7, and 14 with 9 or 5 with 8 in Figure 1F).

Electrophoretic mobility-shift assays (EMSA) demonstrated that in vitro translated Lz can bind specifically to each of the RD binding sites in the SME (Figures 2A–2D). As an in vivo correlate to these experiments, the three RD sites were mutated (5′-RA*AA*RCA-3′) in the context of a transgenic *D-Pax2* rescue construct. Mutation of all three RD binding sites (mRDx3) causes a failure to rescue the *spa^{pol}* eye phenotype (Figure 2E) and D-Pax2 expression in cone cell precursors (Figure 2F). The in vitro and in vivo data together demonstrate that Lz directly regulates *D-Pax2* transcription through the RD binding sites in the SME.

A construct expressing *lacZ* under the control of the SME and the *hsp70* promoter (SME-*lacZ*) faithfully reproduces the wild-type D-Pax2 expression pattern in cone cell precursors (Figure 2G). Mutation of all three RD binding sites in SME-*lacZ* results in the loss of this expression (Figure 2H), further indicating that Lz acts directly through the SME. For the remainder of our analysis, we examined both endogenous D-Pax2 expression as well as SME-*lacZ* expression. In all genetic backgrounds tested, the results obtained in both assays were identical. This suggests that the SME is sufficient for transcriptional regulation of *D-Pax2* in cone cell precursors, and that SME-*lacZ* faithfully reflects this regulation.

The EGFR Pathway Directly Regulates *D-Pax2* Expression in Cone Cell Precursors

In *EGFR^{ts}* third-instar larvae raised at 29°C for 36 hr prior to dissection, D-Pax2 expression is lost in cone cell precursors (Figure 3B). To restrict the loss of EGFR function to the undifferentiated cells posterior to the furrow and cells that acquire their fates during the second phase of morphogenesis, a *lz-Gal4* driver (Crew et al., 1997) was used to express a dominant-negative form of EGFR. In these discs, D-Pax2 expression is lost from cone cell precursors (Figure 3C), while neuronal patterning in the precluster is maintained (Figure 3D). D-Pax2 expression was further examined in mutants of genes encoding the nuclear components of the EGFR signaling pathway, the repressor Yan and the activator PntP2. D-Pax2 expression is also lost in discs in which *lz-Gal4* drives the expression of a nonphosphorylatable form of Yan refractory to the EGFR signal (Figure 3E). Similarly, in the hypomorphic *pnt^{1230}* mutant, a modest reduction of D-Pax2 expression occurs in cone cell precursors (Figure 3F), while a stronger reduction is observed upon expression of a dominant-negative form of PntP2 (Figure 3G). These experiments together suggest that the EGFR signaling pathway activates *D-Pax2* expression in cone cell precursors by relieving Yan-mediated repression and stimulating PntP2 activation.

The above genetic analysis does not address whether the effects of EGFR signaling on *D-Pax2* transcription are direct or indirect. Therefore, we used in vitro mutagenesis to examine potential direct effects. Six ETS domain consensus binding sites (5′-GGAA/T-3′; Nye et al., 1992) were found in the SME (Figure 1F). EMSAs showed that two of these sites (1 and 6, Figures 3H and 3I) are bound by both Yan and PntP2. Yan also binds to two additional sites (2 and 4). All six ETS sites were mutated to 5′-*TT*AA/T-3′ (Wotton et al., 1994) in the context of SME-*lacZ*, and the resulting SME^{mETSx6}-*lacZ* construct was transformed into flies. In these transgenic flies, β-galactosidase expression is lost from cone cell precursors (Figure 3J). Since PntP2 was found to bind only to Ets sites 1 and 6, a SME-*lacZ* construct in which only these sites were mutated (SME$^{mETS(1,6)}$-*lacZ*) was transformed into flies. Figure 3K shows that β-galactosidase expression in cone cells is completely eliminated. These in vitro and in vivo results together demonstrate that PntP2 directly controls *D-Pax2* expression in cone cell precursors by binding to ETS domain sites in the SME. The effect of losing Yan binding in the context of SME^{mETSx6} and SME$^{mETS(1,6)}$ is addressed below.

Notch Signaling Directly Regulates *D-Pax2* Expression in Cone Cell Precursors

In *N^{ts}* third-instar larvae raised at 29°C for 20 hr prior to dissection, D-Pax2 expression is eliminated from cone cell precursors (Figure 4A). Similarly, expression of a dominant-negative form of N under *lz-Gal4* control causes a loss of D-Pax2 expression in cone cell precursors (Figure 4B) without perturbing neuronal development (Figure 4C). D-Pax2 expression is also reduced in discs mutant for *Delta (Dl)* (Figure 4D), which encodes a N ligand. Moreover, expression of a dominant-negative form of Dl (Dl^{DN}) under *lz-Gal4* control causes a loss of D-Pax2 expression in cone cell precursors (Figure 4E), while neuronal patterning occurs in a wild-type fashion (Figure 4F). A further reduction in D-Pax2 expression is seen when Dl^{DN} is driven by *GMR-Gal4* (Figure 4G). A loss of D-Pax2 expression is also seen upon ectopic expression of Hairless (H) (Figure 4H), a direct antagonist of Su(H) function (Brou et al., 1994). These results together suggest that N/Dl signaling via Su(H) is required for proper *D-Pax2* expression in cone cell precursors. This is an inductive rather than lateral inhibitory function

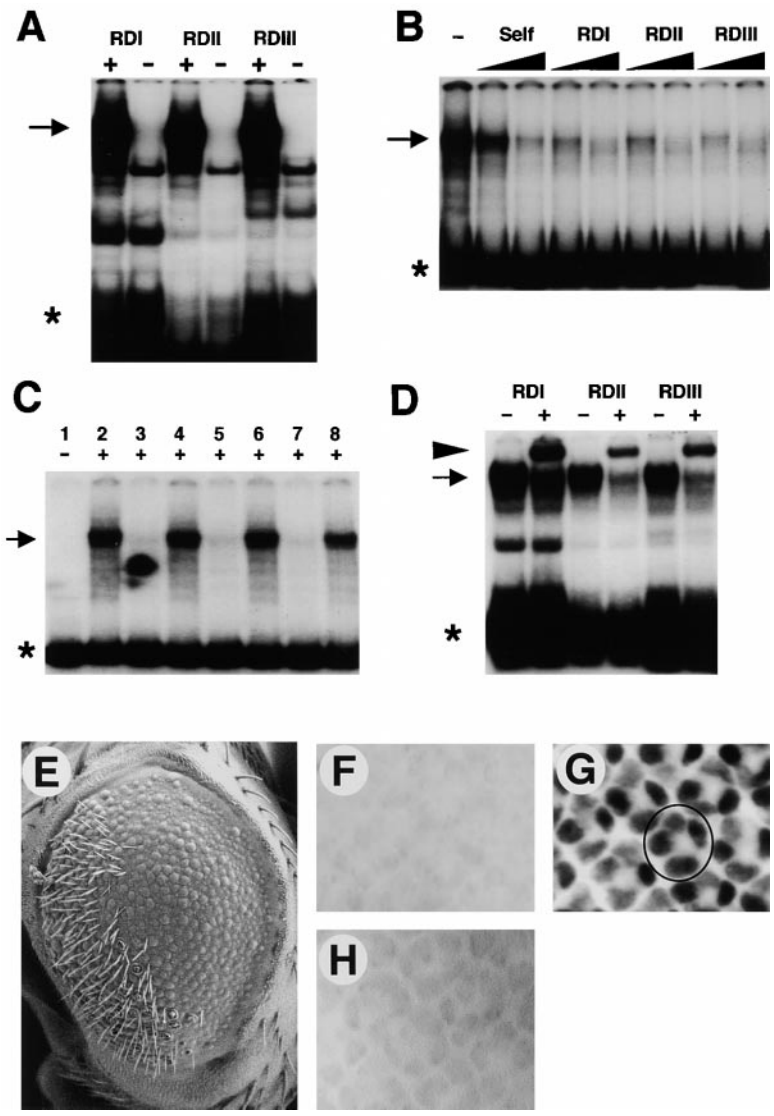

Figure 2. Direct Regulation of *D-Pax2* by Lz

(A–D) Autoradiograms of electrophoretic mobility-shift assays (EMSA). Arrows indicate shifted bands resulting from specific binding of Lz to DNA probes, asterisks mark positions of free probe.

(E) SEM of an adult eye.

(F–H) Immunolocalization of D-Pax2 (F) or β-galactosidase (G and H) in third larval instar eye discs.

(A) EMSA showing binding of Lz to oligonucleotides including one of the three RD binding sites, RDI-RDIII. Lz binds to each oligonucleotide, causing it to migrate more slowly than the free probe. + or − indicates the presence or absence of Lz. Lower molecular weight bands seen in the − lanes are nonspecific.

(B) Competition assay. The probe used for binding in these EMSAs is a SpeI-BglII restriction fragment from the *D-Pax2* eye-specific enhancer (nucleotides 38–320 in Figure 1E) that contains the RDI site. Increased concentrations of cold probe (Self; 10×, 50×) or of oligonucleotides encompassing RDI-RDIII (40×, 200×) efficiently compete with Lz binding.

(C) Competition assays. Cold oligonucleotides including wild-type RDI (lane 3), RDII (lane 5), or RDIII (lane 7) sites, but not oligonucleotides including mutant mRDI (lane 4), mRDII (lane 6), or mRDIII (lane 8) sites, efficiently compete with binding of Lz to the SpeI-BglII probe. + or − indicates presence or absence of Lz. Competitor was omitted in lanes 1 and 2. 200× molar excess of competitor probes was used in lanes 3–8.

(D) Antibody supershift assay. Addition of αLz antibody to the binding reaction of Lz with RD oligonucleotides gives rise to a supershifted band with lower mobility (arrowhead). − or + indicates the absence or presence of αLz antibody.

(E and F) w^{1118}; *P[*mRDx3-*D-Pax2]*; spa^{pol}. In this transformant, all three RD sites in the SpeI fragment are mutated. Neither the spa^{pol} eye phenotype (E) nor D-Pax2 expression in cone cell precursors (F) is rescued (compare with Figures 1G and 1K).

(G) w^{1118}; *P[*SME-*lacZ* w^{+}*]/+*. The expression of the *lacZ* reporter gene under the control of the SME in cone cell precursors (circled) is identical to endogenous wild-type D-Pax2 expression (compare with Figure 1C).

(H) w^{1118}; *P[*SME^{mRDx3}-*lacZ* w^{+}*]*. When the SME is mutated in all three RD sites, expression of β-galactosidase is lost in cone cell precursors.

of the N signaling pathway in cone cell development that has not been previously analyzed with molecular markers. A reporter gene under the transcriptional control of Su(H) binding sites (Go et al., 1998) is expressed in cone cell precursors (Figure 4I), which demonstrates that Su(H) is activated by the N pathway in cone cells.

The Su(H) binding sites in the SME were altered to determine whether the N pathway directly regulates *D-Pax2* transcription. The SME contains eight putative Su(H) binding sites (Figure 1F; 5′-RTGRGAR-3′; Nellesen et al., 1999). EMSAs showed that the Su(H) consensus binding sequence is not strictly followed, since three sites with one mismatch can bind Su(H) (Figure 4J). Su(H) binding is eliminated when the central 5′-GRG-3′ sequence is mutated to 5′-CCC-3′ in all eight sites (Figure 4K). A construct containing these mutations in the context of SME-*lacZ* ($SME^{mSu(H)x8}$-*lacZ*) was transformed into flies. In these transgenic flies, β-galactosidase expression is lost in cone cell precursors (Figure 4L). These in vitro and in vivo results together demonstrate that Su(H) directly controls *D-Pax2* expression in cone cell precursors by binding to the SME.

Single-Cell Clonal Analysis

Mutating Su(H) and ETS binding sites eliminates expression of the target gene in the cone cells, which demonstrates a direct role of these pathways in transcriptional activation of *D-Pax2*. We further used clonal analysis to establish the requirement of the Notch and EGFR pathways in *D-Pax2* expression. Unfortunately, these pathways are necessary for proliferation and have many layers of function (Domínguez et al., 1998, Go et al., 1998). We therefore used a flip-out strategy to inhibit N

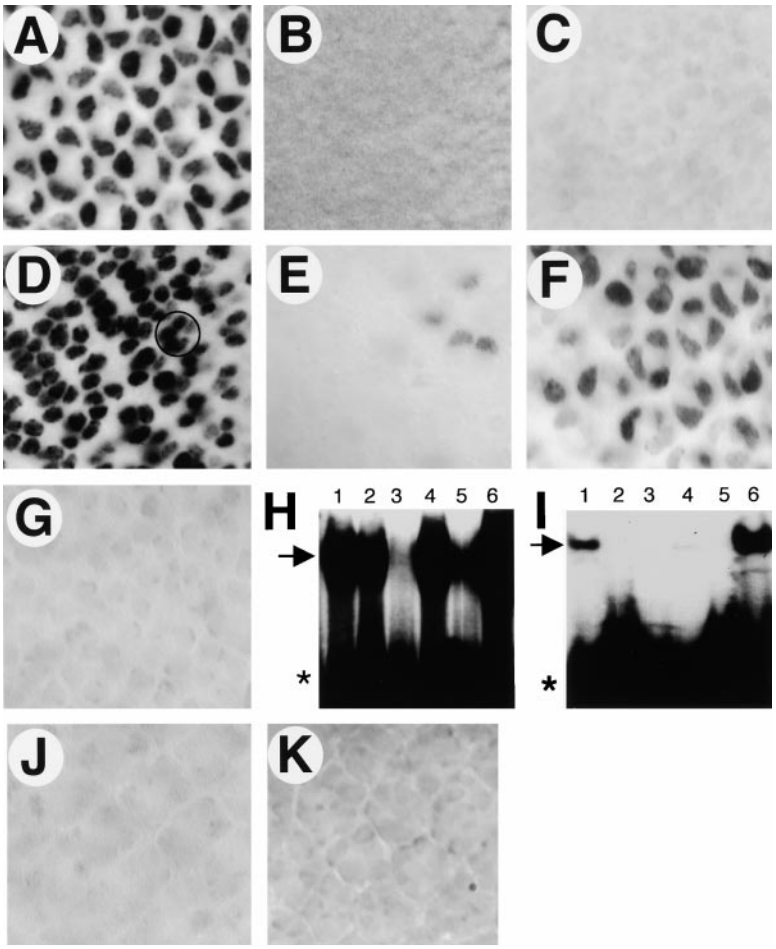

Figure 3. Direct Regulation of D-Pax2 Expression by the EGFR Signaling Pathway

(A–G and J) Immunolocalization of D-Pax2 (A–C and E), ELAV (D), or β-galactosidase (F, G, J, and K) in third larval instar eye discs.

(H and I) EMSA demonstrating specific binding of Yan and PntP2 to the ETS domain binding sites in the SME. Arrows indicate shifted bands caused by binding of ETS domain proteins to DNA probes, asterisks mark free probes.

(A) Wild type. D-Pax2 is expressed in cone cell precursors.

(B) *EGFR^{ts}/EGFR^{top}*. Expression of D-Pax2 is lost from cone cell precursors.

(C) *lz-Gal4:UAS-EGFR^{DN}*. Expression of this dominant-negative form of EGFR under the control of *lz-Gal4* causes a loss of D-Pax2 expression from cone cell precursors.

(D) *lz-Gal4:UAS-EGFR^{DN}*. Expression of the neuronal marker ELAV indicates that neuronal patterning in the precluster (circled) is maintained in the same genotype as in (C).

(E) *lz-Gal4:UAS-yan^{Act}*. Expression of this nonphosphorylatable form of Yan refractory to the EGFR signal leads to a severe reduction of D-Pax2 expression in cone cell precursors.

(F) *pnt^{1230}/pnt^{1230}*; *P[*SME-*lacZ w^{+}]/+*. Expression of SME-*lacZ* in cone cell precursors is reduced in this hypomorphic *pntP2* mutant.

(G) *lz-Gal4:UAS-pntP2^{T151A}*; *P[*SME-*lacZ w^{+}]/+*. Expression of this nonphosphorylatable, dominant-negative form of PntP2 leads to a severe reduction of SME-*lacZ* expression in cone cell precursors.

(H) Yan binds to ETS domain binding sites 1, 2, 4, and 6 within the SME, causing shifted bands.

(I) PntP2 binds to ETS domain binding sites 1 and 6 within the SME, causing shifted bands.

(J) *w^{1118}*; *[*SME^{mETSx6}-*lacZ, w^{+}]*. When the SME is mutated in all six ETS domain binding sites, cone cell expression of the reporter is lost.

(K) *w^{1118}*; *[*SME$^{mETS(1,6)}$-*lacZ, w^{+}]*. When the SME is mutated in PntP2 binding sites 1 and 6, cone cell expression of the reporter is lost. This demonstrates that regulation by PntP2 is direct.

and EGFR function in GFP-labeled single-cell clones (Ito et al., 1997). This was best achieved in clones induced by *GMR-flp*. The GMR enhancer is only active behind the furrow and only a single cell division takes place in this population of cells. As a result, the clone size is very small. In a wild-type background, single cells marked with GFP express D-Pax2 (Figures 5A and 5B). However, when these single cells also express EGFR^{DN} (n = 120 cells in 10 discs; Figures 5C and 5D) or N^{ECN} (n = 150 cells in 12 discs; Figures 5E and 5F), they do not express D-Pax2. Thus, cone cells need functional Notch and EGFR receptors in order to express D-Pax2.

Lz, EGFR, and Notch Restrict *D-Pax2* Expression to Cone Cell Precursors

The results described so far suggest that *D-Pax2* expression is limited to cells which (1) express Lz, (2) receive a sufficiently strong EGFR signal to both alleviate Yan-imposed repression and stimulate PntP2 activation, and (3) receive a N signal able to stimulate Su(H) activation (Figure 5G). The tripartite control of *D-Pax2* expression in the cone cell precursors requires that they receive all three inputs at the proper time in their development. Lz expression in cone cell precursors has been previously demonstrated (Flores et al., 1998). Consistent with their reception of the EGFR signal (Freeman, 1996; Tio and Moses, 1997), activated MAPK is detected in cone cell precursors at the time when they initiate D-Pax2 expression (Figure 5H). We also found that Dl is expressed in developing photoreceptor clusters at the time when the cone cell precursors express D-Pax2 (Figure 5I). Thus, the neuronal clusters signal through an inductive Dl/N pathway to activate *D-Pax2* expression in the neighboring cone cell precursors. These results suggest that, in addition to expressing Lz, the cone cell precursors receive the EGFR and N signals at the time of fate acquisition and D-Pax2 expression. Presumably, at least one of these three activation mechanisms is lacking in cells that do not express *D-Pax2*. This hypothesis was tested through genetic manipulation of the system.

The Absence of EGFR Activation Prevents *D-Pax2* Expression in Undifferentiated Cells

Undifferentiated cells immediately posterior to the furrow receive the N signal (Matsuno et al., 1997) and express Lz, but they do not express D-Pax2. We hypothesized that the absence of D-Pax2 expression in these

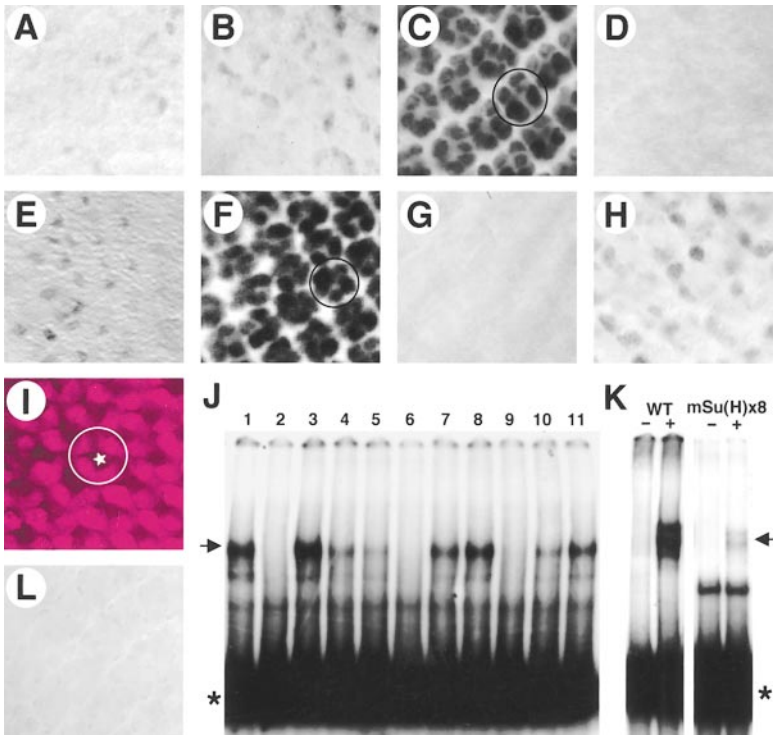

Figure 4. Direct Regulation of D-Pax2 Expression by the N Signaling Pathway

(A–I and L) Immunolocalization of β-galactosidase (A, B, I, and L), ELAV (C and F), or D-Pax2 (D, E, G, and H) in third larval instar eye discs.

(J and K) EMSA demonstrating specific binding of GST-Su(H) to sites in the SME. Arrows indicate shifted bands caused by Su(H) binding to DNA probes, asterisks indicate free probes.

(A) N^{ts1}; *P[*SME-*lacZ* w^+*]*/+. Expression of SME-*lacZ* is lost from cone cell precursors.

(B) *lz-Gal4:UAS-*N^{ECN}; *P[*SME-*lacZ* w^+*]*/+. Expression of this dominant-negative form of N in Lz-expressing cells causes the loss of SME-*lacZ* expression from cone cell precursors.

(C) *lz-Gal4:UAS-*N^{ECN}; *P[*SME-*lacZ* w^+*]*/+. Expression of the neuronal marker ELAV indicates that neuronal patterning in the precluster is maintained (circled) in the same genotype as in (B).

(D) Dl^{B2}/Dl^{R7}. Expression of D-Pax2 is eliminated in cone cell precursors in this heteroallelic *Dl* loss-of-function combination.

(E) *lz-Gal4:UAS-*Dl^{DN}. Expression of this dominant-negative form of Dl causes a reduction of D-Pax2 expression from cone cell precursors.

(F) *lz-Gal4:UAS-*Dl^{DN}. Expression of the neuronal marker ELAV indicates that neuronal patterning in the precluster (circled) is maintained in the same genotype as in (E).

(G) *GMR-Gal4:UAS-*Dl^{DN}. GMR-Gal4 driving the expression of dominant-negative Dl in all cells posterior to the furrow causes a complete loss of D-Pax2 expression.

(H) *lz-Gal4:UAS-H*. Expression of H, an antagonist of Su(H), leads to a reduction of D-Pax2 expression in cone cell precursors.

(I) *12xSu(H)bs-lacZ*. In this construct, twelve copies of Su(H) binding sites control expression of *lacZ*. The observed expression of β-galactosidase indicates that Su(H) functions as a transcriptional activator in cone cell precursors. A single ommatidium is circled showing expression in the four cone cell precursors but not in the neuronal cells (asterisk).

(J) Competition assay. Su(H) binding to the SME in the absence (lane 1) or presence (lanes 2–11) of cold competitors: lanes 2 and 3, wild-type (m4S2) and mutant version (m4S2m) of a known Su(H) binding site, respectively; lanes 4–11, putative Su(H) binding sites found in the SME. Oligonucleotides containing Su(H) sites 2, 3, 4, 6 and 7 (lanes 5, 4, 6, 9, and 10, respectively) efficiently compete for Su(H) binding even though sites 4 and 7 are one nucleotide off the consensus, while site 5 (lane 7; one nucleotide off consensus) and sites 1 and 8 (lanes 8 and 11, respectively; two nucleotides off consensus) do not significantly compete for binding.

(K) Su(H) binding to the SME. − or + indicates absence or presence of Su(H) protein in each assay. Su(H) binds to the wild-type SME (WT). This binding is virtually eliminated when all eight Su(H) binding sites are mutated (mSu(H)x8).

(L) w^{1118}; *P[*$SME^{mSu(H)x8}$*-lacZ, w*$^+$*]* eye discs. When the SME is mutated in all eight Su(H) binding sites, β-galactosidase expression is lost from the cone cell precursors (compare with Figure 2G), which demonstrates that regulation of D-Pax2 by Su(H) is direct.

cells is caused by a lack of the EGFR signal. This hypothesis is consistent with the observation that EGFR signaling causes these cells to differentiate (Xu and Rubin, 1993; Freeman, 1996; Tio and Moses, 1997). Indeed, D-Pax2 is ectopically expressed in undifferentiated cells that express an activated form of EGFR (Figure 5J). Loss-of-function yan^{e2D}/yan^{pokX8} discs also show ectopic expression of D-Pax2 in undifferentiated cells (Figure 5K). Similarly, in discs expressing SME^{mETSx6}*-lacZ*, in which the six ETS sites in the SME are mutated, β-galactosidase is also expressed in undifferentiated cells (Figure 5L). Presumably, relief of Yan repression is sufficient to activate some *D-Pax2* in undifferentiated cells. In $SME^{mETS(1,6)}$*-lacZ*,where the Pnt binding sites are eliminated but two of the Yan binding sites are still intact, there is no expression of β-galactosidase in the undifferentiated cells (Figure 5M). These results suggest that while the undifferentiated cells posterior to the furrow express Lz and receive the N signal, they fail to express D-Pax2 because they do not receive the EGFR signal and are therefore unable to relieve the Yan-imposed repression of *D-Pax2*.

The Absence of N Activation Prevents *D-Pax2* Expression in R7

The R7 precursors express Lz and receive RTK signals, yet they do not express D-Pax2. We hypothesized that this is due to the lack of the N signal at the time of R7 determination. Indeed, expression of an activated form of N (N^{act}), leads to ectopic D-Pax2 expression in R7 precursors (Figure 5N), which suggests that D-Pax2 is not normally expressed in R7 because this cell does not receive the N signal. These results are consistent with the previous observation that the R7 cell loses its neuronal characteristics upon expression of N^{act} (Fortini et al., 1993).

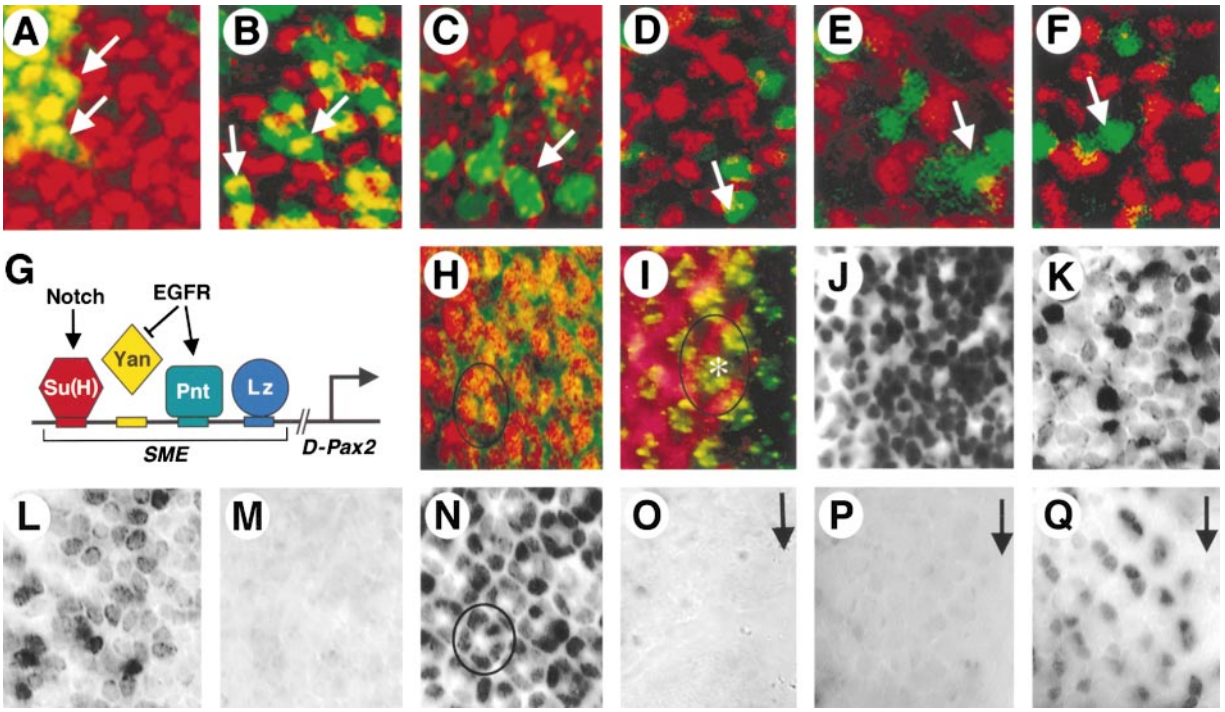

Figure 5. Cell-specificity of D-Pax2 Regulation

(A–F) Clonal analysis of D-Pax2 expression (red) in cone cells. (G) Summary of *D-Pax2* regulation by Lz, EGFR, and N. (H and I) Immunolocalization of β-galactosidase (red) and dpERK (green, H) or Dl (green, I) in third-instar eye discs by confocal microscopy. (J–Q) Immunolocalization of β-galactosidase reporter in third-instar eye discs by light microscopy. Posterior is to the left.

(A) *hsp70-flp*; *Ay-Gal4 UAS-GFP*. Flip-out clone in wild-type eye disc using *hsp*70-*flp*. Cells expressing both GFP and D-Pax2 show yellow nuclei (arrows). Note that GFP (green) is both nuclear and cytoplasmic while D-Pax2 is exclusively nuclear.

(B) *GMR-flp*; *Ay-Gal4 UAS-GFP*. Single-cell flip-out clones in wild-type eye disc (GFP, green) induced by *GMR-flp* and stained with D-Pax2 antibody (red). Cone cells co-expressing GFP and D-Pax2 are yellow (arrows).

(C) *hsp70-flp*; *Ay-Gal4 UAS-GFP*; *UAS-EGFR^{DN}*. Flip-out clones generated at the early third larval instar. No overlap is seen between cells expressing both EGFR^{DN} and GFP (green) and those expressing D-Pax2 (red).

(D) *GMR-flp*; *Ay-Gal4 UAS-GFP*; *UAS-EGFR^{DN}*. Single-cell flip-out clones induced by *GMR-flp* and expressing EGFR^{DN} at the third larval instar. No overlap is seen between cells expressing both EGFR^{DN} and GFP (green) and those expressing D-Pax2 (red). A total of 120 green cells were examined in (C) and (D) at the stage when cone cells develop.

(E) *hsp70-flp*; *Ay-Gal4 UAS-GFP*; *UAS-N^{ECN}*. Flip-out clones generated at the early third larval instar. No overlap is seen between GFP and N^{ECN} expressing cells (green) and D-Pax2 expressing cells (red).

(F) *GMR-flp*; *Ay-Gal4 UAS-GFP*; *UAS-N^{ECN}*. Single-cell flip-out clones induced by *GMR-flp* and expressing N^{DN} at the third larval instar. No overlap is seen between GFP and N^{ECN} expressing cells (green) and D-Pax2 expressing cells (red). A total of 150 green cells were examined in (E) and (F) at the stage when cone cells develop.

(G) Cone cell-specific activation of *D-Pax2* expression is dependent on three inputs: (i) Lz binding to the RD sites in the eye-specific enhancer (SME), (ii) EGFR signal-dependent inactivation of Yan and activation of PntP2, which then binds to ETS domain binding sites in the SME, and (iii) Notch signal-dependent activation of Su(H), which binds to the Su(H) binding sites in the SME.

(H and I) Cone cell precursors receive the proper signals.

(H) SME-*lacZ*. Optical section at the level of cone cell precursors. Activated, phosphorylated MAPK (green) is seen in cone cells, which indicates that these cells receive an RTK signal at the time of SME-*lacZ* (red) expression. Activated MAPK is primarily cytoplasmic; however, small amounts can been seen in nuclei (yellow). A single ommatidium is circled.

(I) SME-*lacZ*. Dl (green) is expressed in photoreceptor clusters (asterisk), but not in cone cells (circled). Expression of this N ligand is downregulated when SME-*lacZ* (red) expression initiates, suggesting transduction of the N signal from the signaling photoreceptor cells to the receiving cone cell precursors.

(J–M) Lack of EGFR signal prevents D-Pax2 expression in undifferentiated cells. The area shown in these three panels is entirely posterior to the furrow.

(J) *lz-Gal4:UAS−λ-topDER*; *P[*SME-*lacZ w^{+}]/+*. Expression of this activated form of EGFR causes ectopic expression of SME-*lacZ* in all of the undifferentiated cells posterior to the furrow.

(K) *yan^{e2D}/yan^{pokx8}*; *P[*SME-*lacZ w^{+}]/+*. SME-*lacZ* is ectopically expressed in undifferentiated cells in this heteroallelic *yan* loss-of-function combination.

(L) *w^{1118}*; *P[*SME^{mETSx6}-*lacZ w^{+}]*. Ectopic expression in undifferentiated cells is evident when all six ETS domain binding sites are mutated in the SME. This demonstrates a direct role for Yan in the negative regulation of *D-Pax2* in the undifferentiated cells.

(M) *w^{1118}*; *P[*SME$^{mETS(1,6)}$-*lacZ w^{+}]*. Ectopic expression in undifferentiated cells is lost when PntP2 binding sites are mutated, but two additional Yan binding sites are maintained. This demonstrates a direct role for Yan in the negative regulation of *D-Pax2* in undifferentiated cells.

(N) Lack of N signal prevents D-Pax2 expression in the R7 precursor. *sev-N^{act}/+*; *P[*SME-*lacZ w^{+}]/+*. Ectopic expression of N^{act} in the R7 precursor leads to expression of SME-*lacZ* in this cell. A representative cluster with five cells expressing β-galactosidase is circled.

(O–Q) Lack of Lz and N signal prevents D-Pax2 expression in the R3/R4 precursors. The furrow is marked with an arrow.

(O) *sev-lz/+*; *P[*SME-*lacZ w^{+}]/+*. Ectopic expression of Lz in the R3 and R4 precursors does not lead to expression of SME-*lacZ* in these cells.

(P) *sev-N^{act}/+*; *P[*SME-*lacZ w^{+}]/+*. Ectopic expression of activated N in the R3 and R4 precursors does not lead to expression of SME-*lacZ* in these cells.

(Q) *sev-lz/+*; *sev-N^{act}/+*; *P[*SME-*lacZ w^{+}]/+*. Coexpression of both Lz and activated N leads to expression of SME-*lacZ* in the R3/R4 precursors (small arrows).

Cell type	Active components			
	N pathway		RTK pathway	
	Lz	Su(H)*	Yan	PntP2*
undiff	Yes	Yes	No	
R3/R4	No	No	Yes	
R7	Yes	No	Yes	
cone	Yes	Yes	Yes	

Figure 6. A Combinatorial Code for Cell Fate Specification

The three components discussed in this paper, Lz, N, and EGFR, can be used to describe the differences between at least four different cell types: cone, R7, R3/R4, and undifferentiated cells. Each of these cell types receives a different combination of signals, which creates the unique set of activated transcription factors that ultimately specify the cell's fate. In such a code, a small number of multifunctional signals such as EGFR and N can be combined to create a large number of distinct cell types (see text for details). Active forms of Su(H) and PntP2 are indicated with an asterisk.

The Absence of N Activation and Lz Prevents *D-Pax2* Expression in R3 and R4

Thus far, this study has focused on cells that express Lz. However, the regulation of *D-Pax2* expression can also be tested in cells that lack Lz, such as the R3/R4 precursors. These cells receive the EGFR signal (Freeman, 1996) but receive the N signal after their initial fate specification, during ommatidial rotation (Cooper and Bray, 1999; Fanto and Mlodzik, 1999). Ectopic expression of either Lz (Figure 5O) or N^{act} (Figure 5P) in the R3/R4 precursors fails to activate *D-Pax2* expression in these cells. However, when Lz and N^{act} are coexpressed in the R3/R4 precursors, D-Pax2 is expressed in these cells (Figure 5Q). These results demonstrate that the lack of both N signaling and Lz during the proper time window prevents R3/R4 cells from expressing *D-Pax2*.

Discussion

In this study, we have examined one example of the complex interplay between multiple signaling pathways during the acquisition of diverse cell fates. We have shown that the nuclear effectors of the EGFR and N signal transduction pathways, Yan, PntP2, and Su(H), and the transcriptional regulator, Lz, act in a combinatorial manner on a tissue-specific enhancer to restrict the expression of *D-Pax2* to the cone cell precursors of the *Drosophila* eye disc. Furthermore, by genetically manipulating these inputs, we observe ectopic expression of *D-Pax2* in specific cell types that do not normally express it. This study provides an exciting example of two multifunctional signaling pathways, EGFR and N, acting together to influence the development of a single cell type. The regulation of *D-Pax2* transcription by each of these inputs is direct, since its expression can be eliminated by mutating the RD, ETS, or Su(H) binding sites in the eye-specific *D-Pax2* enhancer.

The entire code for generating the approximately ten different cell types in the *Drosophila* ommatidium is not yet understood. However, the available data can create a combinatorial code for cell fate specification the use of only three components (Figure 6). In this code, differential activation of the RTK and N signaling cascades creates the unique combinations of activated or inactivated transcription factors that are required for the acquisition of different cell fates. Each of these transcription factors is ubiquitously expressed in the precursor population, but is activated only in cells that receive the proper signals. The model presented in Figure 6 reflects requirements rather than sufficiency for cell fate specification. We anticipate that as additional components are uncovered, the code for the cell types listed in Figure 6 will become complete and that the code for other cell types such as R1/R6 will become evident. In some instances, the regulation of the same target gene may involve different combinations of signals in different cell types. Preliminary data indicate that the combinatorial logic for expression of *D-Pax2* in primary pigment cells is different from that in cone cells in that it requires Su(H) and Lz but not Pnt (G. V. F., R. N., and U. B., unpublished data).

Precise spatial and temporal regulation of the various inputs required for cell fate determination is essential for proper eye patterning. Lz function is restricted to the undifferentiated cells posterior to the furrow by a currently unidentified mechanism. Lozenge might prepare several enhancer regions early, so that they are competent to respond to a later signal. The EGFR ligand, Spitz (Spi), and the N ligand, Dl, are expressed in the previously determined neuronal clusters and act over short extracellular distances at the appropriate time for induction of cone cell fate in the neighboring precursors. Temporal control of the EGFR signal is achieved through the reiterative secretion of Spi as the ommatidium progressively develops (Freeman, 1996; Tio and Moses, 1997). Spi function is spatially restricted by competition with its diffusible antagonist, Argos (reviewed in Freeman, 1997). The N signal is activated early in eye development near the furrow (reviewed in Artavanis-Tsakonas et al., 1999), but this study highlights a late, inductive function of N that is dependent on the temporally controlled expression of Dl in the developing photoreceptor clusters. This N signaling positively influences differentiation and acts in cooperation with, rather than antagonistically to, the EGFR pathway. Tethering of Dl to the membrane allows only adjacent cells to receive this N signal (reviewed in Artavanis-Tsakonas et al., 1999).

Numerous studies involving promoter analysis have established that combinations of multiple transcription factor binding sites are important for gene activation. Comprehensive in vivo studies of the regulatory regions of the sea urchin *Endo 16* gene (Arnone and Davidson, 1997; Yuh et al., 1998) and the *Drosophila even-skipped* (*eve*) stripe 2 enhancer (Arnosti et al., 1996), for example, have convincingly demonstrated the importance of both positive and negative inputs in controlling gene activity. Our studies have focused on the integration of local signaling cascades in the regulation of a target gene. Our aim was to understand the molecular details, in the in vivo context of a developing animal, of how combinatorial signaling can generate fine differences in fate amongst cells that are initially equivalent and that communicate through local cell–cell interactions. Any one signal may not impart fate-specifying information when acting alone, but in combination, different signals can create unique sets of activated transcription factors at

the correct time and in a cell occupying a specific position. Although we have unraveled the molecular mechanisms involved in the regulation of only a single gene, it is likely that the other cell-specific transcription factors expressed in the eye disc and in other contexts will be controlled in a similar manner. Indeed, an example of direct integration of signaling pathways has been observed in muscle differentiation (Halfon et al., 2000 [this issue of *Cell*]). Moreover, analysis of the *pros* enhancer in the *Drosophila* eye suggests that similar combinations of signaling pathways and transcription factors operate in the regulation of this gene in R7 and cone cells (Xu et al., 2000 [this issue of *Cell*]). As additional controlling regions are analyzed, different combinations of signaling systems will undoubtedly be uncovered. Nevertheless, we anticipate that the total number of inputs will not be very large.

Experimental Procedures

Clonal Analysis

Flip out clones expressing *UAS-EGFR*^{DN} or *UAS-N*^{ECN} were generated by the use of the *Ay-Gal4* system (Ito et al., 1997) and marked with *UAS-GFP*, both inserted on the 2nd chromosome. Clones in eye discs were created by *hsp*70-*flp* or *GMR-flp*. *hsp*70-*flp* crosses were maintained at 18°C; early third-instar larvae were heat shocked at 37°C for 20 min to generate small clones.

Constructs Used for Germline Transformation

The 926 bp SpeI fragment of intron 4 of *D-Pax2* (Figure 1E) and its truncated versions were cloned into the BamHI site of the *spa*-PCG2 vector (Fu and Noll, 1997). Fragments 1–14 (Figure 1F) were derived from the SpeI (Figure 1E) fragment by PCR (nucleotide positions in intron 4 are in parentheses): 1 (59–813), 2 (59–519), 3 (59–411), 4 (158–813), 5 (359–813), 6 (158–519), 7 (158–411), 8 (359–519), 9 (213–519), 10 (281–519), 11 (158–474), 12 (158–438), 13 (59–474), and 14 (213–813). Each of the 15 *D-Pax2* transgenes, driven by their own promoter and the 15 different eye enhancer fragments (Figure 1F), were assayed as single copies for rescue of the *spa*^{pol} eye phenotype and D-Pax2 expression in cone cell precursors in several independent transgenic lines. The rescue efficiency of the *spa*^{pol} eye phenotype indicated in Figure 1F is the average of all independent lines of each transgene, which showed the following distributions (numbers indicate number of independent lines with weak (+), partial (++), and full (wt) rescue, respectively). SpeI, constructs 1, 2, 4, and 6: all lines are wt; construct 3: 2, 3, and 1; construct 5: 15, 3, and 0; construct 7: 4, 8, and 3; construct 8 with NotI ends: 6, 2, and 0 (with BamHI ends: 11, 6, and 3); construct 9: 0, 8, and 3; construct 10: 0, 6, and 4; construct 11: 0, 6, and 2; construct 12: 0, 9, and 2; construct 13: 0, 4, and 1; and construct 14: 0, 8, and 0. All homozygous viable ++ lines, but none of the + lines, rescue the *spa*^{pol} eye phenotype when two copies of the transgene are present.

SME-*lacZ*, SME^{mRDx3}-*lacZ*, SME^{mETSx6}-*lacZ*, SME$^{mETS(1,6)}$-*lacZ*, and SME$^{mSu(H)x8}$-*lacZ* were generated by amplifying the appropriate 158–519 fragments and cloning them into PwHZ128, which contains the *hsp70* promoter and the bacterial *lacZ* gene (a gift from A. Courey).

mRDx3 and mETSx6 were generated by site-directed mutagenesis as described (Huang et al., 1993). To generate mSu(H)x8, in vitro mutagenesis for Su(H)3, 6, and 7 was performed as above. The remaining Su(H) sites were altered on the mutated Su(H)3, 6, and 7 template using a PCR-based strategy.

Acknowledgments

We thank H. Wang for extensive help with fly genetics and transformations, J. Jackson and S. Robert for assistance with making constructs, T. Gutjahr for help with SEM, and F. Ochsenbein for help with graphics. We are indebted to R. Carthew for sharing reagents and results prior to publication. We thank S. Artavanis-Tsakonas, N. Baker, R. Carthew, A. Courey, M. Freeman, E. Hafen, Y. Hiromi, C. Klämbt, Z.-C. Lai, M. Mlodzik, K. Moses, M. Muskavitch, J. Pollock, I. Rebay, G. Rubin, D. Yamamoto, L. Zipursky, and K. Matthews and the Bloomington Stock Center for fly stocks and reagents. We thank A. Courey, H. Herschman, M. Levine, S. L. Zipursky, and members of the Banerjee laboratory for critical comments on the manuscript. G. V. F. was supported by a USPHS National Research Service Award (GM07195). This work was supported by the Swiss National Science Foundation (Grant 31-40874.94 to M. N.), the Kanton Zürich, the NIH (Grant # 2R01EY08152 to U. B.), and a McKnight Foundation Investigator Award to U. B.

Received November 29, 1999; revised August 22, 2000.

References

Arnone, M.I., and Davidson, E.H. (1997). The hardwiring of development: organization and function of genomic regulatory systems. Development *124*, 1851–1864.

Arnosti, D.N., Barolo, S., Levine, M., and Small, S. (1996). The *eve* stripe 2 enhancer employs multiple modes of transcriptional synergy. Development *122*, 205–214.

Artavanis-Tsakonas, S., Rand, M.D., and Lake, R.J. (1999). Notch signaling: cell fate control and signal integration in development. Science *284*, 770–776.

Ausubel, F.M., Brent, R., Kingston, R.E., Moore, D.D., Seidman, J.G., Smith, J.A., and Struhl, K., eds. (1991). Current Protocols in Molecular Biology (New York: John Wiley & Sons).

Bae, S.-C., and Ito, Y. (1999). Regulation mechanisms for the heterodimeric transcription factor, PEBP2/CBF. Histol. Histopathol. *14*, 1213–1221.

Baker, N.E., and Rubin, G.M. (1989). Effect on eye development of dominant mutations in the *Drosophila* homologue of the EGF receptor. Nature *340*, 150–153.

Baker, N.E., and Rubin, G.M. (1992). *Ellipse* mutations in *Drosophila* homologue of the EGF receptor affect pattern formation, cell division, and cell death in eye imaginal discs. Dev. Biol. *150*, 381–396.

Basler, K., Yen, D., Tomlinson, A., and Hafen, E. (1990). Reprogramming cell fate in the developing *Drosophila* retina: transformation of R7 cells by ectopic expression of *rough*. Genes Dev. *4*, 728–739.

Brou, C., Logeat, F., Lecourtois, M., Vandekerckhove, J., Kourilsky, P., Schweisguth, F., and Israël, A. (1994). Inhibition of the DNA-binding activity of *Drosophila* Suppressor of Hairless and of its human homolog, KBF2/RBP-J$_K$, by direct protein-protein interaction with *Drosophila* Hairless. Genes Dev. *8*, 2491–2503.

Brunner, D., Dücker, K., Oellers, N., Hafen, E., Scholz, H., and Klämbt, C. (1994). The ETS domain protein Pointed-P2 is a target of MAP kinase in the Sevenless signal transduction pathway. Nature *370*, 386–389.

Cagan, R.L., and Ready, D.F. (1989). *Notch* is required for successive cell decisions in the developing *Drosophila* retina. Genes Dev. *3*, 1099–1112.

Cooper, M.T.D., and Bray, S.J. (1999). Frizzled regulation of Notch signalling polarizes cell fate in the *Drosophila* eye. Nature *397*, 526–530.

Crew, J.R., Batterham, P., and Pollock, J.A. (1997). Developing compound eye in *lozenge* mutants of *Drosophila*: Lozenge expression in the R7 equivalence group. Dev. Genes Evol. *206*, 481–493.

Czerny, T., Bouchard, M., Kozmik, Z., and Busslinger, M. (1997). The characterization of novel *Pax* genes of the sea urchin and *Drosophila* reveal an ancient evolutionary origin of the *Pax2/5/8* subfamily. Mech. Dev. *67*, 179–192.

Daga, A., Karlovich, C.A., Dumstrei, K., and Banerjee, U. (1996). Patterning of cells in the *Drosophila* eye by Lozenge, which shares homologous domains with AML1. Genes Dev. *10*, 1194–1205.

Dickson, B., Sprenger, F., and Hafen, E. (1992). Prepattern in the developing *Drosophila* eye revealed by an activated torso-sevenless chimeric receptor. Genes Dev. *7*, 2327–2339.

Domínguez, M., and de Celis, J.F. (1998). A dorsal/ventral boundary established by Notch controls growth and polarity in the *Drosophila* eye. Nature *396*, 276–278.

Domínguez, M., Wasserman, J.D., and Freeman, M. (1998). Multiple functions of the EGF receptor in *Drosophila* eye development. Curr. Biol. *8*, 1039–1048.

Fanto, M., and Mlodzik, M. (1999). Asymmetric Notch activation specifies photoreceptors R3 and R4 and planar polarity in the *Drosophila* eye. Nature *397*, 523–526.

Flores, G.V., Daga, A., Kalhor, H.R., and Banerjee, U. (1998). Lozenge is expressed in pluripotent precursor cells and patterns multiple cell types in the *Drosophila* eye through the control of cell-specific transcription factors. Development *125*, 3681–3687.

Fortini, M.E., Rebay, I., Caron, L.A., and Artavanis-Tsakonas, S. (1993). An activated Notch receptor blocks cell-fate commitment in the developing *Drosophila* eye. Nature *365*, 555–557.

Freeman, M. (1996). Reiterative use of the EGF receptor triggers differentiation of all cell types in the *Drosophila* eye. Cell *87*, 651–660.

Freeman, M. (1997). Cell determination strategies in the *Drosophila* eye. Development *124*, 261–270.

Fu, W., and Noll, M. (1997). The *Pax2* homolog *sparkling* is required for development of cone and pigment cells in the *Drosophila* eye. Genes Dev. *11*, 2066–2078.

Fu, W., Duan, H., Frei, E., and Noll, M. (1998). *shaven* and *sparkling* are mutations in separate enhancers of the *Drosophila Pax2* homolog. Development *125*, 2943–2950.

Go, M.J., Eastman, D.S., and Artavanis-Tsakonas, S. (1998). Cell proliferation control by Notch signaling in *Drosophila* development. Development *125*, 2031–2040.

Gupta, B.P., and Rodrigues, V. (1995). Distinct mechanisms of action of the *lozenge* locus in *Drosophila* eye and antennal development are suggested by the analysis of dominant enhancers. J. Neurogenet. *10*, 137–151.

Halfon, M.S., Carmena, A., Gisselbrecht, S., Sackerson, C.M., Jimenez, F., Baylies, M.K., and Michelson, A.M. (2000). Ras pathway specificity is determined by the integration of multiple signal-activated and tissue-restricted transcription factors. Cell *103*, this issue, 63–74.

Higashijima, S., Kojima, T., Michiue, T., Ishimaru, S., Emori, Y., and Saigo, K. (1992). Dual *Bar* homeo box genes of *Drosophila* required in two photoreceptor cells, R1 and R6, and primary pigment cells for normal eye development. Genes Dev. *6*, 50–60.

Huang, J.-D., Schwyter, D.H., Shirokawa, J.M., and Courey, A.J. (1993). The interplay between multiple enhancer and silencer elements defines the pattern of *decapentaplegic* expression. Genes Dev. *7*, 694–704.

Ito, K., Awano, W., Suzuki, K., Hiromi, Y., and Yamamoto, D. (1997). The *Drosophila* mushroom body is a quadruple structure of clonal units each of which contains a virtually identical set of neurones and glial cells. Development *124*, 761–771.

Kamachi, Y., Ogawa, E., Asano, M., Ishida, S., Murakami, Y., Satake, M., Ito, Y., and Shigesada, K. (1990). Purification of a mouse nuclear factor that binds to both the A and B cores of the polyomavirus enhancer. J. Virol. *64*, 4808–4819.

Kauffmann, R.C., Li, S., Gallagher, P.A., Zhang, J., and Carthew, R.W. (1996). Ras1 signaling and transcriptional competence in the R7 cell of *Drosophila*. Genes Dev. *10*, 2167–2178.

Kavaler, J., Fu, W., Duan, H., Noll, M., and Posakony, J.W. (1999). An essential role for the *Drosophila Pax2* homolog in the differentiation of adult sensory organs. Development *126*, 2261–2272.

Kimmel, B.E., Heberlein, U., and Rubin, G.M. (1990). The homeo domain protein *rough* is expressed in a subset of cells in the developing *Drosophila* eye where it can specify photoreceptor cell subtype. Genes Dev. *4*, 712–727.

Kumar, J., and Moses, K. (1997). Transcription factors in eye development: a gorgeous mosaic? Genes Dev. *11*, 2023–2028.

Kumar, J.P., Tio, M., Hsiung, F., Akopyan, S., Gabay, L., Seger, R., Shilo, B.-Z., and Moses, K. (1998). Dissecting the roles of the *Drosophila* EGF receptor in eye development and MAP kinase activation. Development *125*, 3875–3885.

Lawrence, P.A., and Green, S.M. (1979). Cell lineage in the developing retina of *Drosophila*. Dev. Biol. *71*, 142–152.

Lesokhin, A.M., Yu, S.-Y., Katz, J., and Baker, N.E. (1999). Several levels of EGF receptor signaling during photoreceptor specification in wild-type, *Ellipse*, and null mutant *Drosophila*. Dev. Biol. *205*, 129–144.

Lindsley, D.L., and Zimm, G.G. (1992). The Genome of *Drosophila melanogaster*. (San Diego: Academic Press).

Matsuno, K., Go, M.J., Sun, X., Eastman, D.S., and Artavanis-Tsakonas, S. (1997). Suppressor of Hairless-independent events in Notch signaling imply novel pathway elements. Development *124*, 4265–4273.

Nellesen, D.T., Lai, E.C., and Posakony, J.W. (1999). Discrete enhancer elements mediate selective responsiveness of *Enhancer of split* Complex genes to common transcriptional activators. Dev. Biol. *213*, 33–53.

Nye, J.A., Petersen, J.M., Gunther, C.V., Jonsen, M.D., and Graves, B.J. (1992). Interaction of murine Ets-1 with GGA-binding sites establishes the ETS domain as a new DNA-binding motif. Genes Dev. *6*, 975–990.

O'Neill, E.M., Rebay, I., Tjian, R., and Rubin, G.M. (1994). The activities of two Ets-related transcription factors required for *Drosophila* eye development are modulated by the Ras/MAPK pathway. Cell *78*, 137–147.

Papayannopoulos, V., Tomlinson, A., Panin, V.M., Rauskolb, C., and Irvine, K.D. (1998). Dorsal-ventral signaling in the *Drosophila* eye. Science *281*, 2031–2034.

Ready, D.F., Hanson, T.E., and Benzer, S. (1976). Development of the *Drosophila* retina, a neurocrystalline lattice. Dev. Biol. *53*, 217–240.

Rebay, I., and Rubin, G.M. (1995). Yan functions as a general inhibitor of differentiation and is negatively regulated by activation of the Ras1/MAPK pathway. Cell *81*, 857–866.

Tio, M., and Moses, K. (1997). The *Drosophila* TGFα homolog Spitz acts in photoreceptor recruitment in the developing retina. Development *124*, 343–351.

Tomlinson, A., and Ready, D.F. (1987). Neuronal differentiation in the *Drosophila* ommatidium. Dev. Biol. *120*, 366–376.

Wolff, T., and Ready, D.F. (1991). The beginning of pattern formation in the *Drosophila* compound eye: the morphogenetic furrow and the second mitotic wave. Development *113*, 841–850.

Wotton, D., Ghysdael, J., Wang, S., Speck, N.A., and Owen, M.J. (1994). Cooperative binding of Ets-1 and core binding factor to DNA. Mol. Cell. Biol. *14*, 840–850.

Xu, T., and Rubin, G.M. (1993). Analysis of genetic mosaics in developing and adult *Drosophila* tissues. Development *117*, 1223–1237.

Xu, C., Kauffmann, R.C., Zhang, J., Kladny, S., and Carthew, R.W. (2000). Overlapping activators and repressors delimit transcriptional response to receptor tyrosine kinase signals in the *Drosophila* eye. Cell *103*, this issue, 87–97.

Yuh, C.-H., Bolouri, H., and Davidson, E.H. (1998). Genomic cis-regulatory logic: experimental and computational analysis of a sea urchin gene. Science *279*, 1896–1902.

Zipursky, S.L., and Rubin, G.M. (1994). Determination of neuronal cell fate: lessons from the R7 neuron of *Drosophila*. Ann. Rev. Neurosci. *17*, 373–397.